

THERMAL LOAD DETERMINATION FOR THE FATIGUE ANALYSIS OF THE SURGE LINE

M.H.C. Hannink¹

¹ Consultant, NRG PALLAS, Petten, The Netherlands (hannink@nrg.eu)

ABSTRACT

Thermal loads are important in the fatigue assessment of nuclear power plant (NPP) components. Some NPPs are equipped with dedicated fatigue monitoring systems to measure these loads. However, fatigue monitoring systems are not present in all NPPs, and in some cases, data are required at locations that are difficult to access. This paper, therefore, focusses on the determination of thermal loads using measurement data from operational process monitoring systems (PMS), which are available at all NPPs. The study concentrates on the surge line of a typical pressurized water reactor, a highly relevant location for fatigue in the primary system. Simulations of thermal loads were validated for transients of representative events, and the sensitivity of the results to various parameters was investigated. It can be concluded that the simplified finite element (FE) model that was introduced and validated in Hannink and Uitslag-Doolaard (2022) is suitable for simulating temperature fluctuations in the surge line. However, using measurement data from an operational PMS as input for model requires great care and does not yield accurate results over long periods of time with the simulation method presented in this paper. For shorter periods of time and smaller fluctuations in the pressurizer water level, the approach has the potential to provide rough estimates of temperature fluctuations for design analyses.

INTRODUCTION

Fatigue is an important degradation mechanism for components of nuclear power plant (NPPs). Cyclic loads on piping and nozzles are often caused by temperature fluctuations. Design analyses frequently include overly conservative assumptions for these thermal loads. If environmentally assisted fatigue is considered, or if the expected numbers of cycles increase as NPPs enter long-term operation, such overly conservative assumptions can make it challenging to maintain compliance with design criteria. Because more and more NPPs enter long-term operation, detailed understanding of the thermal loads on NPP components is becoming increasingly important. Temperature measurements associated with thermal loads can enhance this understanding. Some NPPs are equipped with dedicated fatigue monitoring systems. However, fatigue monitoring systems are not present in all NPPs, and in some cases, data are required at locations that are difficult to access. This paper, therefore, focusses on the determination of thermal loads using measurement data from operational process monitoring systems (PMS), which are available at all NPPs. The study concentrates on the surge line of a typical pressurized water reactor, a highly relevant location for fatigue in the primary system.

In prior work, an approach was presented to simulate temperature fluctuations in the surge line of an NPP using measurement data from an operational PMS (Hannink (2024)). The validation of the calculated temperatures in the structure showed promising results for the analysed events. However, results were still sensitive to the initial conditions and the heat transfer coefficients of the applied convection boundary conditions. The current paper presents an investigation of the appropriate selection of these parameters, along with further validation using additional transients of representative events.

FINITE ELEMENT MODEL

The study was conducted on the surge line of a typical pressurized water reactor (Hannink (2024), Hannink and Uitslag-Doolaard (2022), Uitslag-Doolaard et al. (2019)). The geometry of the configuration is shown in Figure 1. The model included the pipes as well as the nozzles at the pressurizer and the main coolant line. The pipes had an inner diameter of 315 mm and consisted of 20-mm-thick low-alloy steel with a 5-mm-thick austenitic stainless steel cladding. The thermal loads in the surge line were simulated using a structural thermal finite element (FE) model. The structure was meshed with hexahedral eight-node thermal solid elements (Figure 1). The cladding and thermal sleeves were explicitly included in the model. The analyses were performed using the FE software ANSYS 2022 R1.

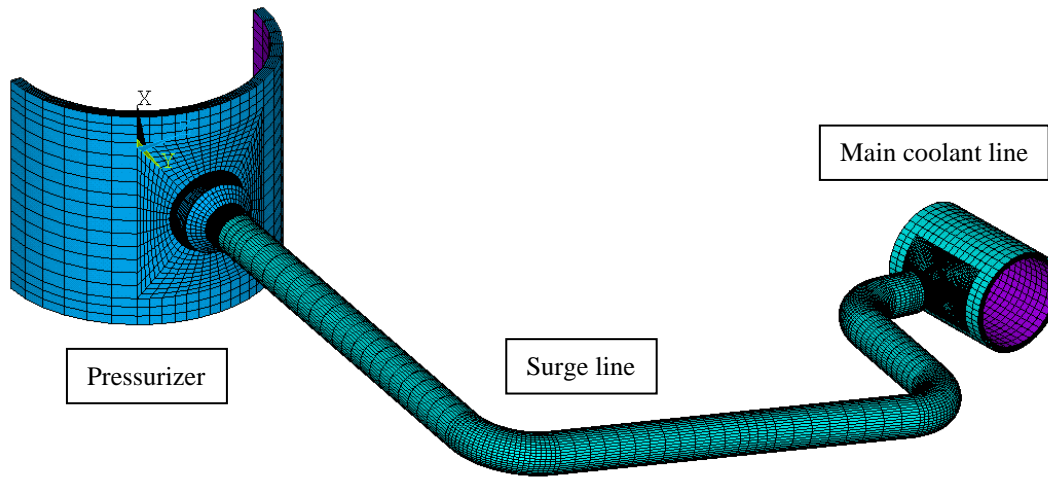


Figure 1. FE model of the surge line and the nozzles at the pressurizer and the main coolant line.

THERMAL LOADS

Load cases which often lead to fatigue-relevant loading of the surge line are start-ups, shutdowns, scrams and pump trips. Large temperature fluctuations, generally, occur due to start-ups and shutdowns. During normal operation, the surge line is partially filled with warmer water from the pressurizer and cooler water from the main coolant line (see example in Figure 2). During start-ups and shutdowns, the water temperatures in the pressurizer and the main coolant line change in a step-wise manner (see example in Figure 3). The differences between the temperature levels as shown in Figure 3 determine the magnitude of the temperature fluctuations. During an insurge event, cooler water from the main coolant line (blue in Figure 2) flows towards the pressurizer, so the pipe cools down. During an outsurge event, warmer water from the pressurizer (red in Figure 2) flows towards the main coolant line, so the pipe heats up.

THERMAL LOAD MODELLING

Approach

The thermal loads in the surge line were modelled in the same way as presented in Hannink (2024), where the temperature fluctuations were simulated by applying a convection boundary condition to the inner wall of the pipe. The exterior of the configuration was assumed to be fully insulated (adiabatic). The convection boundary condition at the inner wall of the pipe was defined by a time-dependent bulk temperature and a constant heat transfer coefficient.

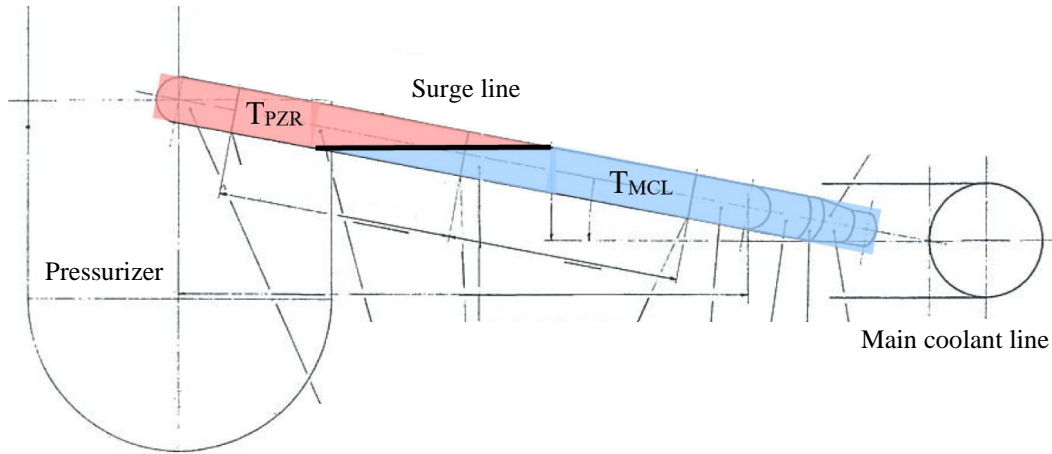


Figure 2. Thermal load in the surge line (side view).

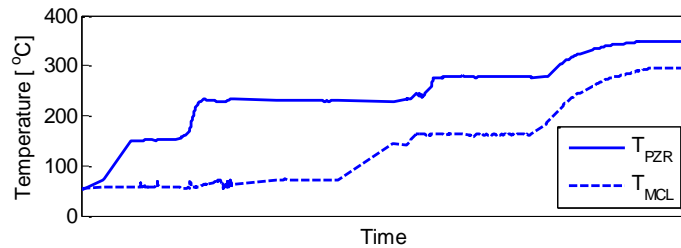


Figure 3. Temporal profiles of the water temperatures in the pressurizer (T_{PZR}) and the main coolant line (T_{MCL}) during a start-up.

Bulk Temperature

To model the bulk temperature, part of the water in the surge line was assumed to have the same temperature as the water in the pressurizer (T_{PZR} , red in Figure 2), and part of the water in the surge line was assumed to have the temperature of the main coolant (T_{MCL} , blue in Figure 2). The temperatures of the pressurizer water and the main coolant were obtained from measurements by the operational PMS, and were functions of time. In this paper, two events are analysed. Both are parts of start-ups after refuelling outages. The measured temperature signals of the two events are shown in Figure 4. The interface between the warmer (pressurizer) and cooler (main coolant) water was assumed to be a horizontal plane (see Figure 2) and was modelled as a step change in temperature (i.e., no mixing taking place). Insurge and outsurge events were simulated by moving the interface through the pipe.

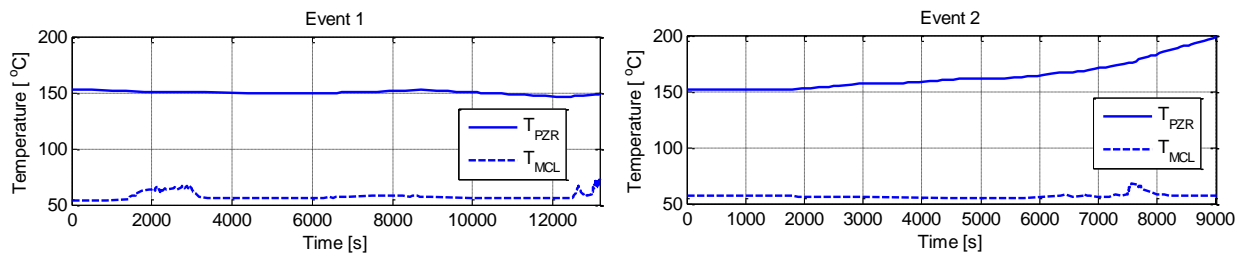


Figure 4. Measured water temperatures in the pressurizer (T_{PZR}) and the main coolant line (T_{MCL}).

The position of the interface in the surge line was defined by the coordinate x (see Figure 1) and was derived from measurements of the water level in the pressurizer (see Figure 5, top). First, the changes in water volume in the pressurizer were calculated from the measurement signals. Second, the shift of the interface position in the surge line due to these changes in water volume in the pressurizer was calculated.

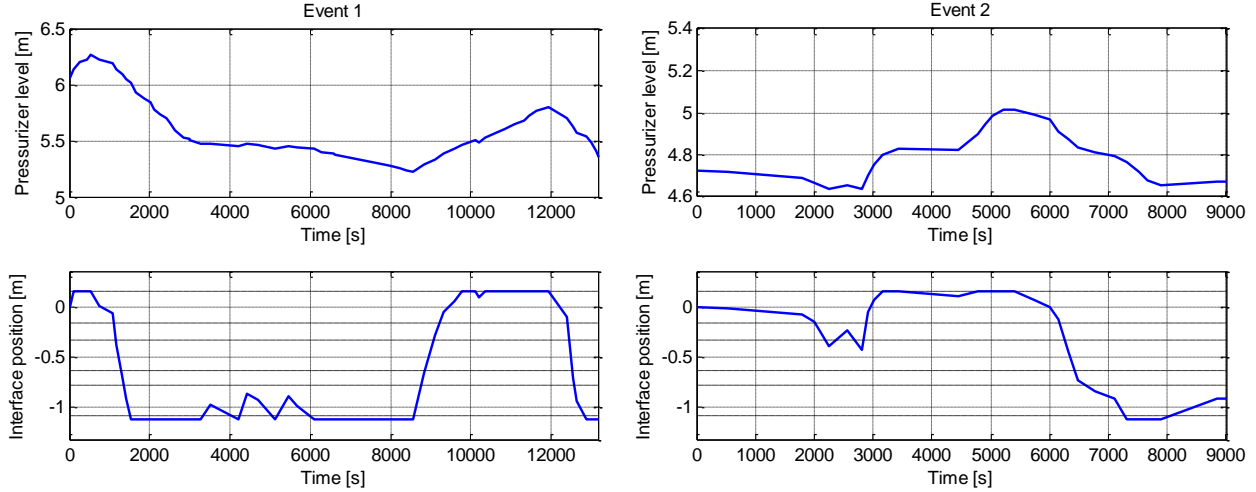


Figure 5. Measured pressurizer level L and derived interface position x as a function of time.

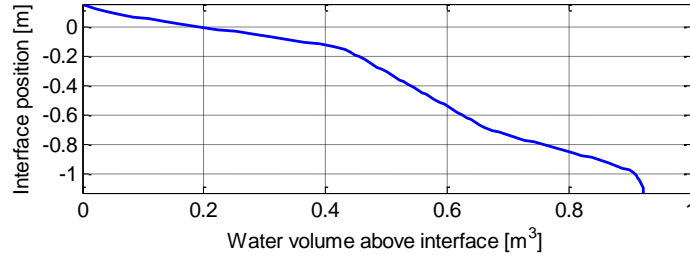


Figure 6. Volume of the water in the surge line above the interface for interface positions x .

Figure 6 shows the volume of the water in the surge line above the interface for all possible interface positions. This is the water with temperature T_{PZR} . If the interface is at the top, the surge line is completely filled with main coolant. If the interface is at the bottom, the surge line is completely filled with pressurizer water. The water volume above the interface at start time t_0 , $V(x(t_0))$, was determined by linear interpolation of the data in Figure 6 using the assumed starting position $x(t_0)$ of the interface. Determination of the starting position of the interface is discussed in more detail in the section Initial Conditions below. Subsequently, a lookup table was created with volume differences ΔV for time t_1 by subtracting $V(x(t_0))$ from the volume in Figure 6. The interface position $x(t_1)$ at time t_1 was then determined by linear interpolation of the data in the lookup table. The quantity $\Delta V(t_1)$ was calculated with the following equation:

$$\Delta V(t_{i+1}) = [L(t_{i+1}) - L(t_i)]\pi \left(\frac{D_{PZR}}{2}\right)^2 \quad (1)$$

where is D_{PZR} the diameter of the pressurizer, and L is the pressurizer water level obtained from PMS readings (see Figure 5). The above steps were repeated to find the interface positions at the other time steps. Figure 5 shows the resulting interface positions as functions of time for the two events analysed in this

paper. If the measured volume differences led to interface positions outside the surge line, the interface positions were kept constant at the highest and lowest values of x , as appropriate.

Heat Transfer Coefficients

The heat transfer coefficients were determined by an empirical convection correlation for a fully developed turbulent flow in a cylindrical pipe (Incropera and DeWitt, 1990). One of the parameters in the convection correlation is the Reynolds number. The Reynolds number depends on the velocity v with which the water moves back and forth through the surge line. In Hannink (2024), it was shown that the calculated thermal loads are sensitive to the applied heat transfer coefficients. Two cases were investigated in the paper. In the first case, the heat transfer coefficients were defined as functions of time, with the velocity v derived from the measurements of the pressurizer water level L (see Figure 5, top). The velocity v of the water in the surge line was calculated as follows:

$$v(t) = \frac{dL}{dt} \frac{D_{PZR}^2}{D_{SL}^2} \quad (2)$$

where D_{PZR} is the inner diameter of the pressurizer, and D_{SL} is the inner diameter of the surge line. Different heat transfer coefficients were determined for the surge line regions with pressurizer and main coolant temperatures T_{PZR} and T_{MCL} . In the second case, the heat transfer coefficients were kept constant at the maximum value of the heat transfer coefficients determined in the first case. The same heat transfer coefficient was used for the entire configuration. It was demonstrated that the second case led to better results for the analysed events. Constant maximum values of the heat transfer coefficients were, therefore, used for the analyses in the current paper as well.

The heat transfer coefficient calculations were performed using temperature- and pressure-dependent water properties (Lemmon et al., 2021). The temperatures and the pressures were taken from the PMS readings in the pressurizer and the main coolant line, and were taken as constant, time-averaged values. The resulting maximum heat transfer coefficients were 938 W/(m²K) for Event 1 and 306 W/(m²K) for Event 2.

Loading Conditions in the Pressurizer and the Main Coolant Line

The thermal loads in the pressurizer and main coolant line were also simulated using convection boundary conditions. The bulk temperatures in the pressurizer and main coolant line were as shown in Figure 4. The heat transfer coefficients were set to the same constant values as the heat transfer coefficients in the surge line.

INITIAL CONDITIONS

As mentioned in the Introduction section, validation of the approach presented above for modelling thermal loads based on PMS readings showed promising results for the analysed events in Hannink (2024). It was also concluded, however, that the results were still sensitive to the initial conditions. In an attempt to

develop a guideline for determining the starting position of the interface between the warmer and cooler water in the surge line, many fatigue-relevant events were analysed. In many instances it was found that when simulating, for example, a full start-up, global changes in pressurizer level are larger than the total volume of the surge line. With the applied simulation technique, this would mean that the interface would move out of the surge line, and that the surge line would be completely filled with warmer water from the pressurizer or with cooler water from the main coolant line. From practical experience it is known, however, that this is rarely the case, which makes it difficult to precisely track the position of the interface over long periods of time. Another reason that makes it difficult to precisely track the position of the

interface over long periods of time is that the PMS readings occasionally contain measurement errors. For shorter periods of time (in the order of a few hours), reasonably good results can be obtained, as demonstrated in the next section. However, also for these events, no universal set of guidelines was found for determining the starting position of the interface based only on PMS readings.

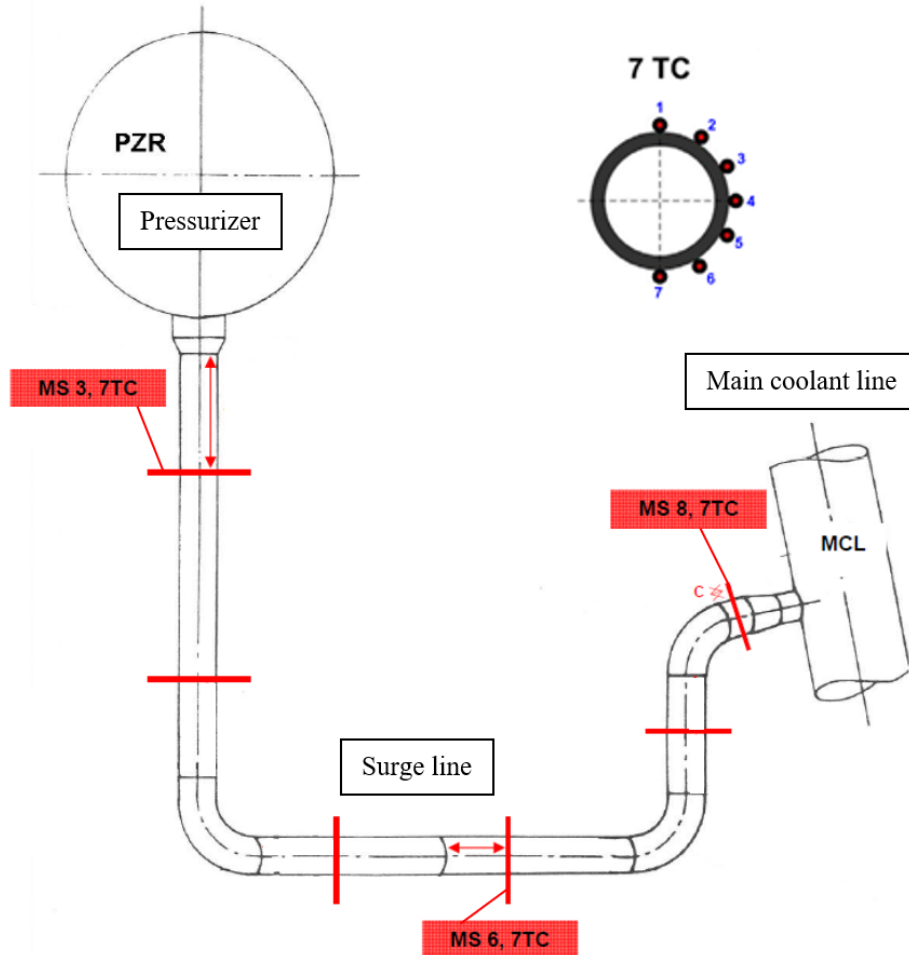


Figure 7. Positions of measurement sections (MS) and thermocouples (TC) of the fatigue monitoring system.

THERMAL ANALYSIS RESULTS

The temperatures in the surge line due to the applied thermal loads were calculated by performing transient thermal analyses. To verify to what extent the simulated thermal loads correspond to reality, the calculated temperatures in the surge line were compared to the temperatures measured by a dedicated fatigue monitoring system. It should be noted that the data from this fatigue monitoring system were only used for validation purposes, and not for modelling thermal loads. The presented thermal load modelling method only uses operational PMS data. For validation, fatigue monitoring data of three measurement sections (MS) were available: one near the pressurizer nozzle, one on the inclined part of the surge line, and one near the main coolant line nozzle (MS 3, MS 6, and MS 8, respectively, see Figure 7). Each measurement section contains seven thermocouples attached to the outer wall of the pipe (TC, see Figure 7).

Figure 8 to Figure 13 show the temperatures calculated at these positions together with the temperatures measured by the fatigue monitoring system. The results are plotted for the seven thermocouple positions of each measurement section. Analyses were performed for two different resolutions of the measurements of the pressurizer water level. The left figures show the results for the cases where resolution of the water level signal was variable, determined by a smart storing algorithm (measurements in Figure 5). The right figures show the results for the cases where the water level signal had a resolution of 5 seconds.

DISCUSSION

Figure 8 to Figure 13 show that the global trends of the temperature fluctuations are simulated reasonably well. For Event 1, the simulated stratification profiles improve when high-resolution water level signals are used to determine the position of the interface between warmer and cooler water in the surge line (see Figure 8 to Figure 10, right versus left). The signals contain more noise, though, which could be reduced by filtering. For Event 2, simulation of the stratification profiles at MS 3 and MS 8 improves slightly when the resolution of the water level measurements is increased (see Figure 11 to Figure 13, right versus left). However, the effect is less pronounced than for Event 1.

The FE model contains several simplifications. One of the simplifications is that the FE analyses start from a steady-state situation, whereas the measurements of the fatigue monitoring system start from transient states. These differences in initial conditions partially explain the initial mismatches in temperature distributions over the circumference of the pipe. Another simplification in the current model is the absence of a mixing layer between the warmer (pressurizer) and cooler (main coolant) water. The calculated and measured stratification profiles, therefore, somewhat differ. Improvement could be obtained by including a mixing layer in the FE model.

As was demonstrated in Hannink (2024), the calculated thermal loads are sensitive to the selection of the heat transfer coefficients. The calculated heat transfer coefficients vary considerably over time. Because derivatives of the water level measurements in the pressurizer are used to determine the velocity v of the water, the accuracy of the heat transfer coefficients also depends on the resolution of the pressurizer level measurements. The simulations to generate the results in Figure 8 to Figure 13 (right versus left) used the same values of the heat transfer coefficients, so the effect of the measurements resolution on the heat transfer coefficients is not demonstrated in the results presented in this paper.

Figure 11 to Figure 13, show that the increases in simulated temperatures at MS 6 and MS 8 (blue lines) occur slightly later than in reality (black lines). This lag can be explained by the calculated, delayed drop of the interface, as shown in Figure 5, bottom right.

CONCLUSION

In Hannink (2024), an approach was presented to simulate thermal loads in the surge line of an NPP using measurement data from an operational PMS. The validation of the calculated temperatures in the structure showed promising results for the analysed events. However, results were still sensitive to the initial conditions and the heat transfer coefficients of the applied convection boundary conditions. In the current paper, the approach was further validated by analysing additional events of longer duration.

Several fatigue-relevant events were analysed in an attempt to develop a guideline for determining the initial conditions. In many instances it was found that large global changes in pressurizer level and measurement errors make it difficult to precisely track the position of the interface between the warmer and cooler water in the surge line over long periods of time and accurately simulate the thermal loads. For

shorter periods of time (in the order of a few hours), it was demonstrated that reasonably good results can be obtained, though a meaningful guideline for the initial conditions is still challenging to define. In addition to the initial conditions, the resolution of the water level measurements in the pressurizer was demonstrated to affect the accuracy of the simulation results.

Generally, it can be concluded that the simplified FE model that was introduced and validated in Hannink and Uitslag-Doolaard (2022) is suitable for simulating temperature fluctuations in the surge line. From the work in the current paper and Hannink (2024), it can be concluded that using measurement data from an operational PMS as input for model requires great care and does not yield accurate results over long periods of time with the simulation method presented in this paper. For shorter periods of time and smaller fluctuations in the pressurizer water level, the approach has the potential to provide rough estimates of temperature fluctuations for design analyses.

REFERENCES

- Hannink, M.H.C. and Uitslag-Doolaard, H.J. (2022). "Modelling of Thermal Loads of the Surge Line of a PWR," *Proc., SMiRT 26*, Berlin/Potsdam, Berlin, Division II.
- Hannink, M.H.C. (2024). "Thermal load determination for fatigue analyses of nuclear power plant components," *Proc., SMiRT 27*, Yokohama, Japan, Division II.
- Incropera, F.P. and DeWitt, D.P. (1990). *Fundamentals of heat and mass transfer, 3rd ed.*, John Wiley & Sons.
- Uitslag-Doolaard, H.J., De Bont, C.G.M., Roelofs, F. and Blom, F.J. (2019). "Combined Thermal-mechanical and Thermal-hydraulic Analyses in a Pressurized Surge line," *Proc., ICAPP*, Juan-les-pins, France, Paper 00161.

Disclaimer

Goods labelled with an EU DuC (European Dual-use Codification) not equal to 'N' are subject to European and national export authorization when exported from the EU and may be subject to national export authorization when exported to another EU country as well. Even without an EU DuC, or with EU DuC 'N', authorization may be required due to the final destination and purpose for which the goods are to be used. No rights may be derived from the specified EU DuC or absence of an EU DuC.

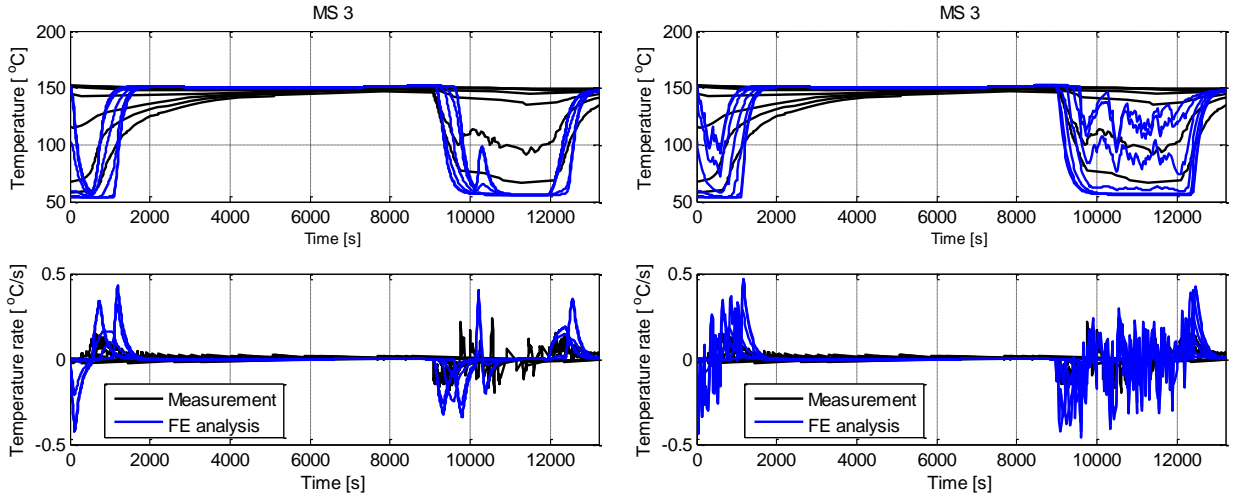


Figure 8. Temperatures at the thermocouple positions of MS 3 during Event 1.

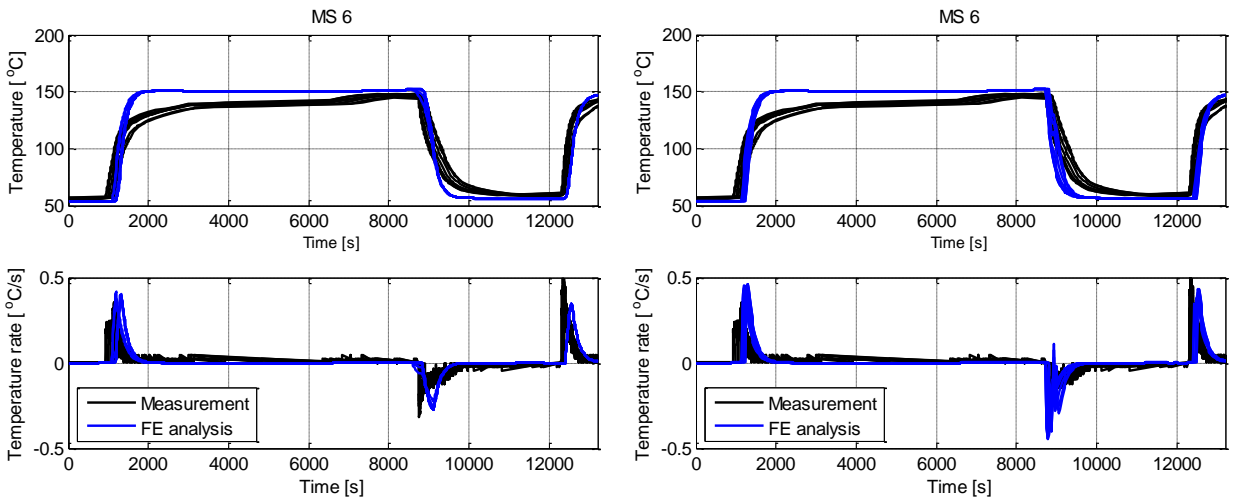


Figure 9. Temperatures at the thermocouple positions of MS 6 during Event 1.

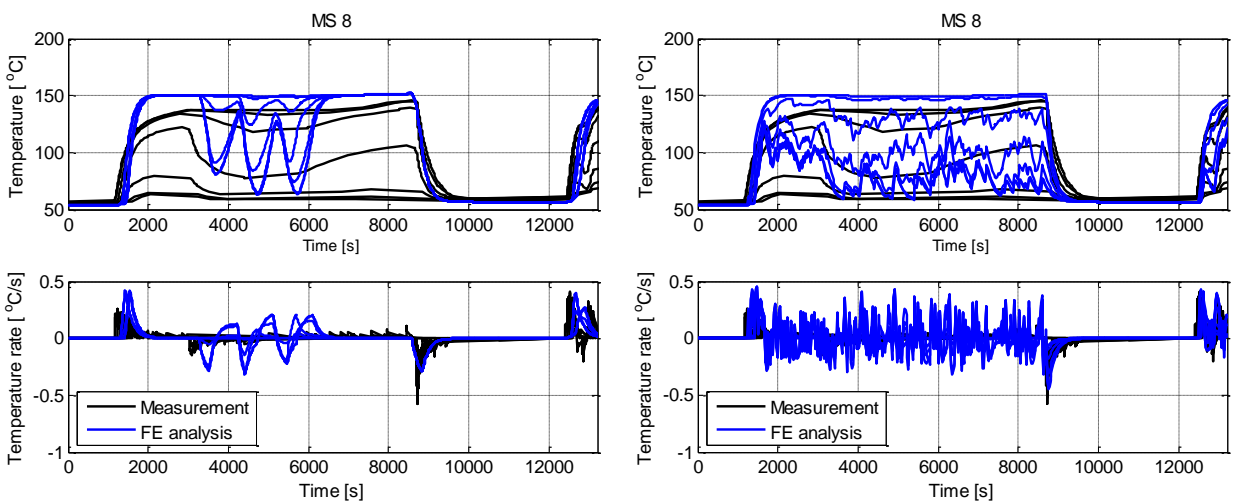


Figure 10. Temperatures at the thermocouple positions of MS 8 during Event 1.

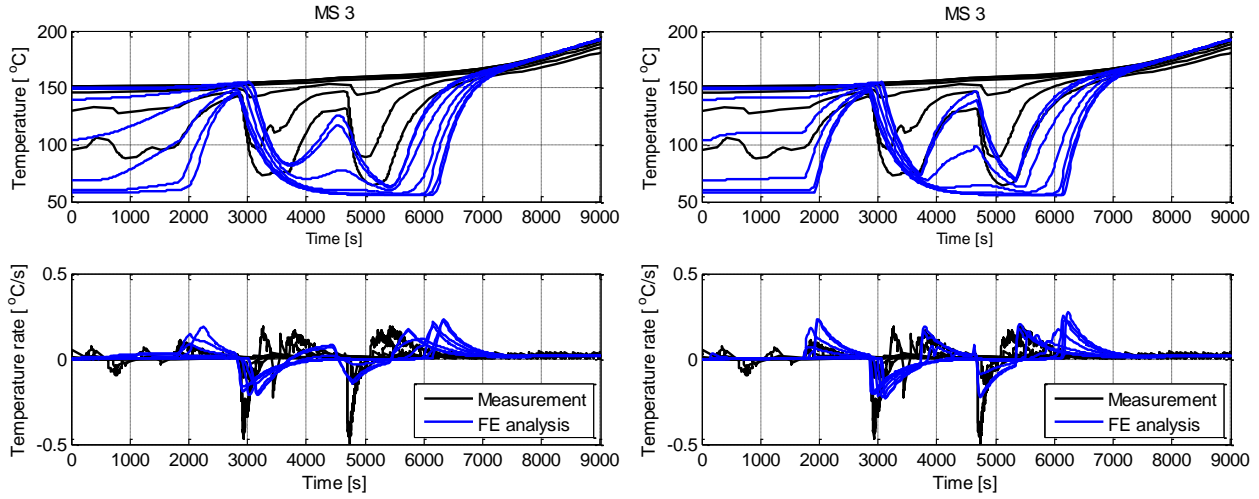


Figure 11. Temperatures at the thermocouple positions of MS 3 during Event 2.

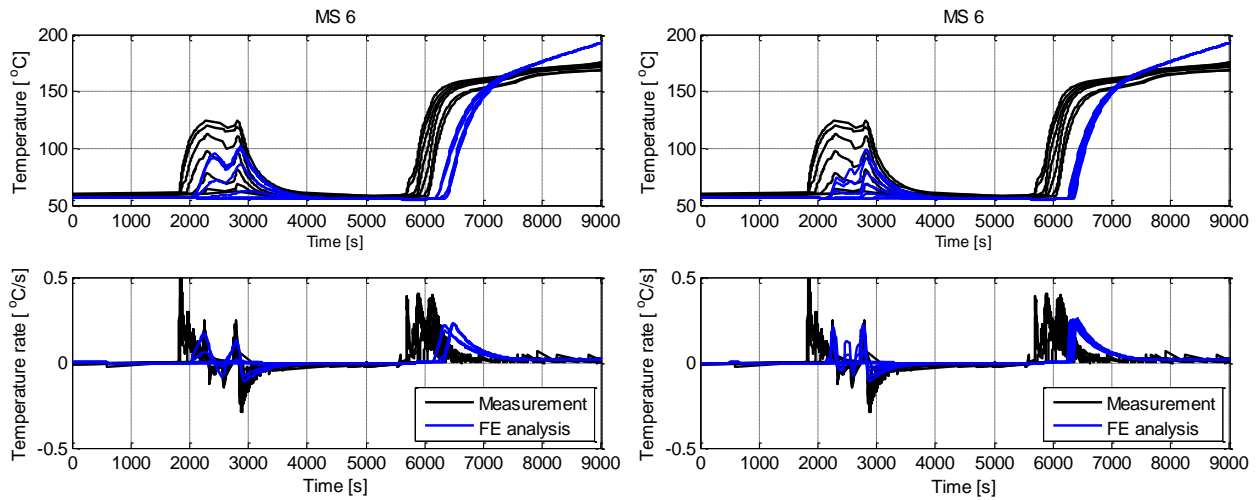


Figure 12. Temperatures at the thermocouple positions of MS 6 during Event 2.

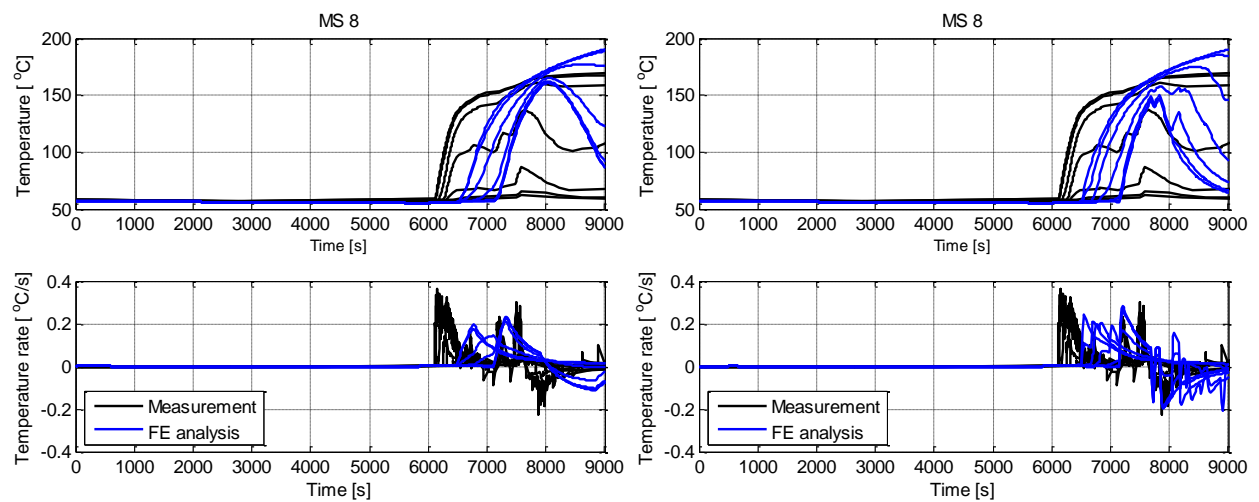


Figure 13. Temperatures at the thermocouple positions of MS 8 during Event 2.